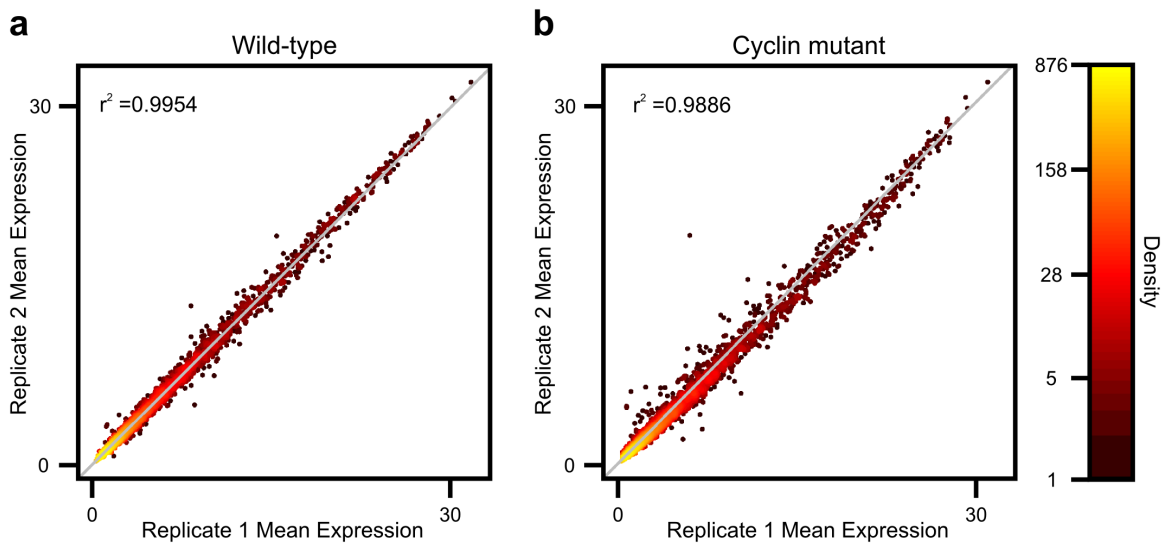

Figure S1 | **Reproducibility of replicate experiments.** Scatter plots of mean normalized absolute expression levels over all timepoints within an experiment for each mapped probe for both **a**, wild-type and **b**, cyclin-mutant cells. Each probe's X and Y coordinate is defined by its mean normalized absolute expression/1000 in replicate 1 and 2, respectively. A linear model was fit to each plot (gray line) and adjusted r^2 values are given. To more clearly reveal the density of points near the origin, each point is colored according to the number of other points contained within a square of length 500 centered on that point.

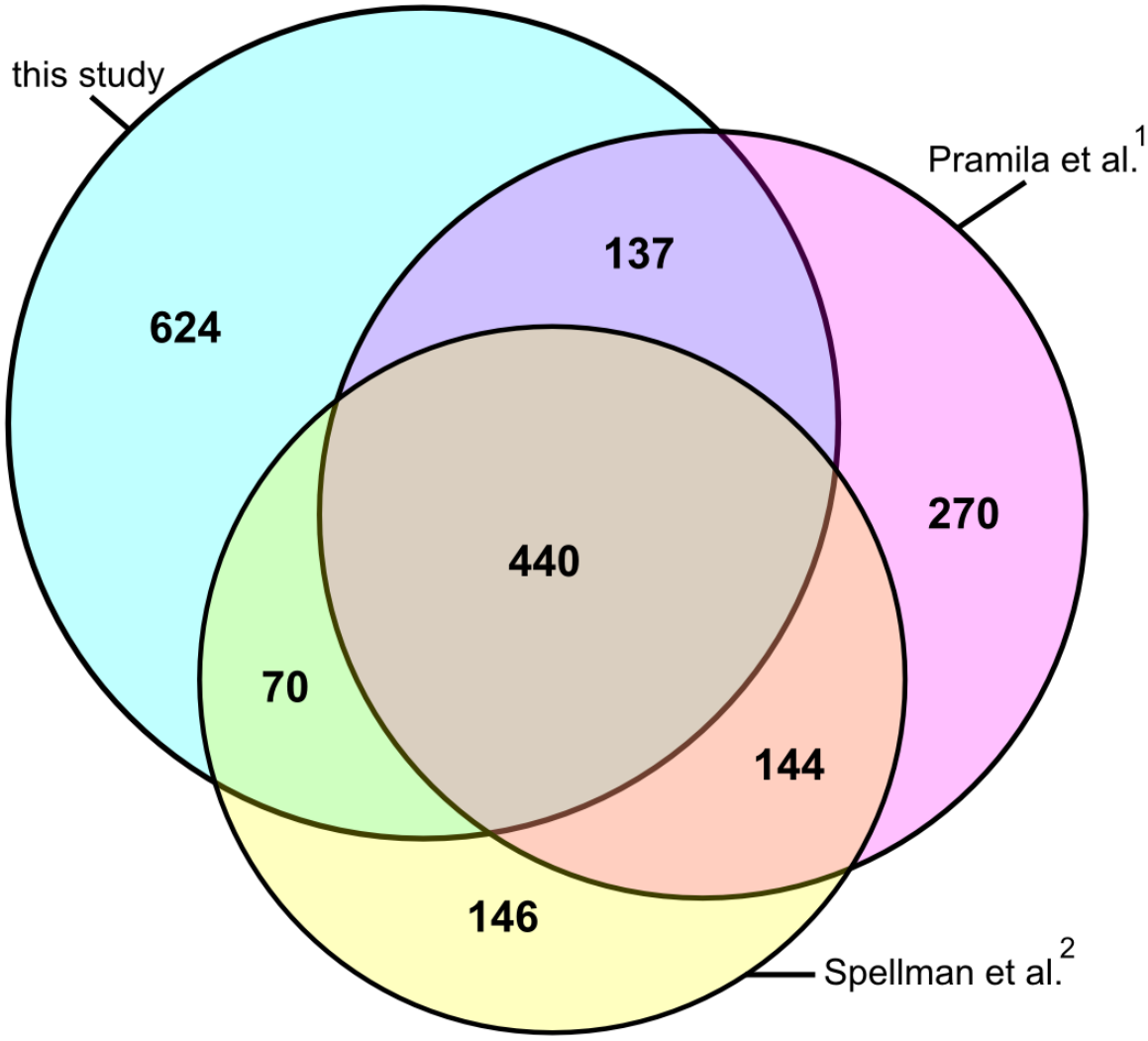

Figure S2 | **Comparison of periodic genes identified by three studies.** A Venn diagram of the overlap between the 1271 unique genes identified as periodic in wild-type cells by this study, the 991 from Pramila et al.,[1] and the 800 from Spellman et al.[2] The set of 991 periodic genes from Pramila et al. contains all those with PBM5 rankings of 1000 or less, from the three datasets available at `http://www.fhcrc.org/science/labs/breeden/cellcycle/`. The set of 800 periodic genes from Spellman et al. was obtained directly from `http://genome-www.stanford.edu/cellcycle/data/rawdata/CellCycle95.xls`. See Supplementary Table 2 for more information on the wild-type consensus set (WTCON) of 440 genes identified as periodic by all three studies.

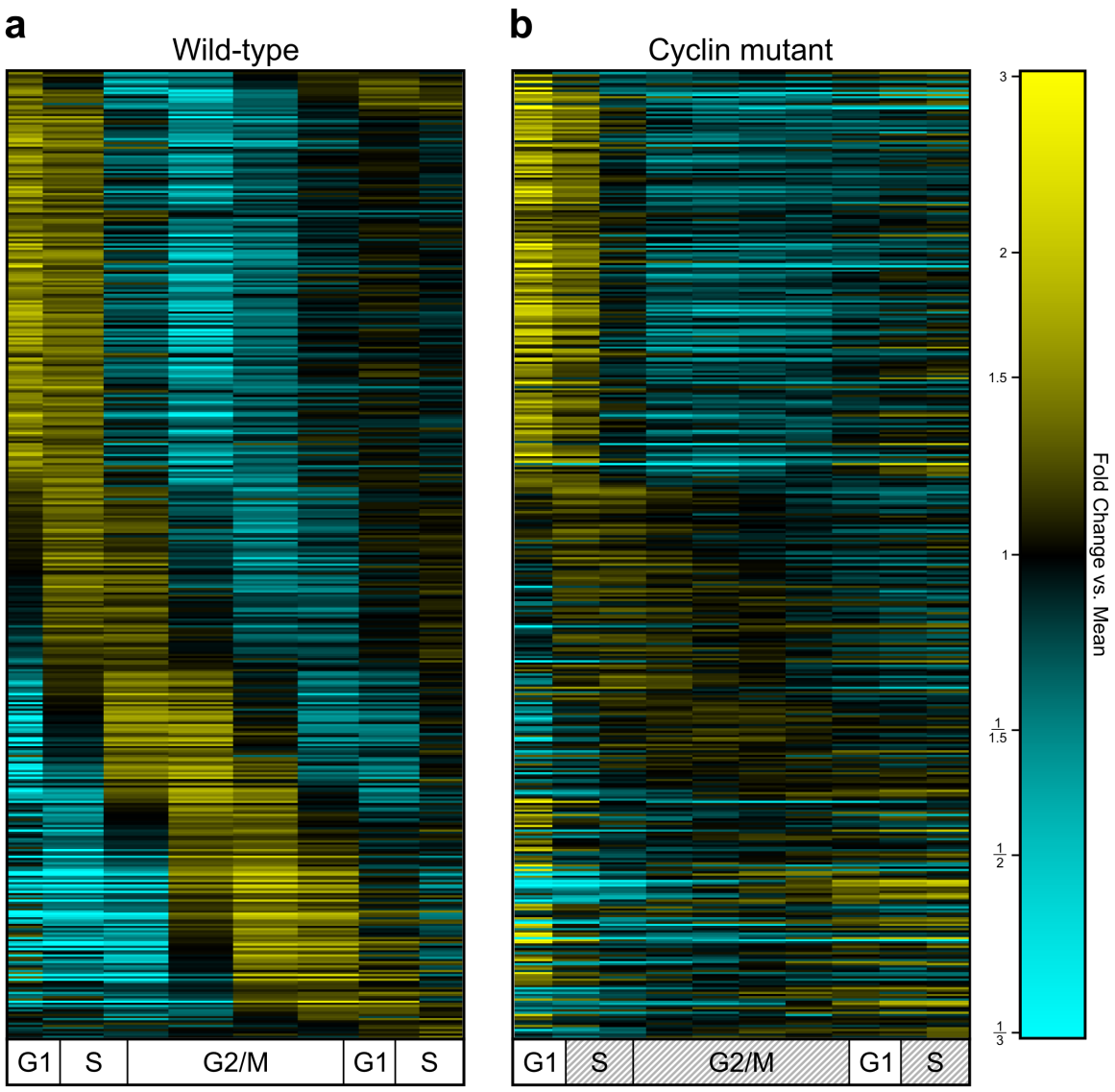

Figure S3 | **Cell cycle dynamics of consensus periodic genes (WTCON) in wild-type and cyclin-mutant cells.** Heatmaps depicting mRNA levels of the 440 genes in WTCON are shown for **a**, wild-type and **b**, cyclin-mutant cells. Each row in **a** and **b** represents data for the same gene (ordered gene names are listed in Supplementary Table 2). Transcript levels are expressed as log2-fold change vs. mean expression. Transcript levels at each of the points in the time series were mapped onto a cell-cycle timeline.[3] The S phase and G2/M phases of the cyclin-mutant timeline are shaded to indicate that by conventional definitions, cyclin-mutant cells do not enter S phase or mitosis.

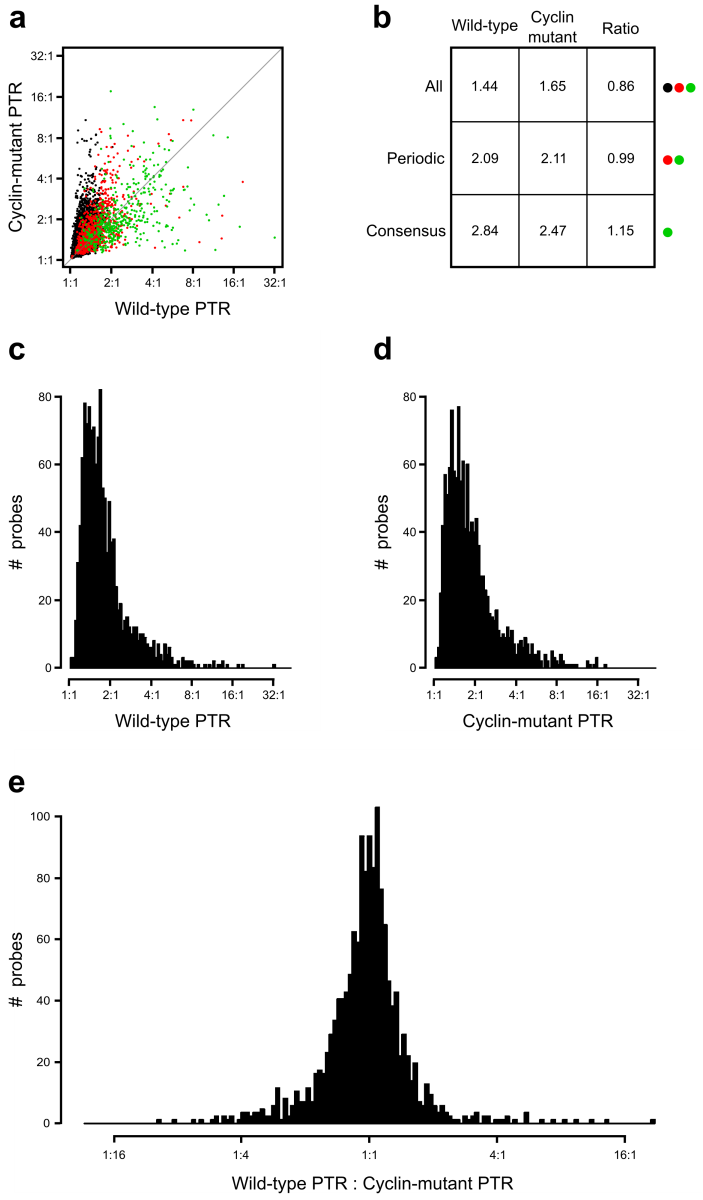

Figure S4 | **Peak to trough ratio for all genes.** **a**, The average wild-type peak to trough ratio (PTR, see Supplementary Section 4) (x-axis) is plotted against the average cyclin-mutant PTR (y-axis) for each gene/probe identified as periodic by all three studies (green, see Supplementary Fig. 2)[1,2], by this study only (red), or not identified as periodic by this study (black). **b**, The average PTR in wild-type (Column 1) or cyclin-mutant cells (Column 2), as well as the average wild-type to cyclin-mutant PTR ratio (Column 3). Colored dots to the right indicate which genes from (**a**) are included in each calculation. A histogram of the average PTR for each of the WTPER genes in **c**, wild-type and **d**, cyclin-mutant cells. **e**, Histogram of ratios of the PTRs of each WTPER gene in wild-type vs. cyclin-mutant cells.

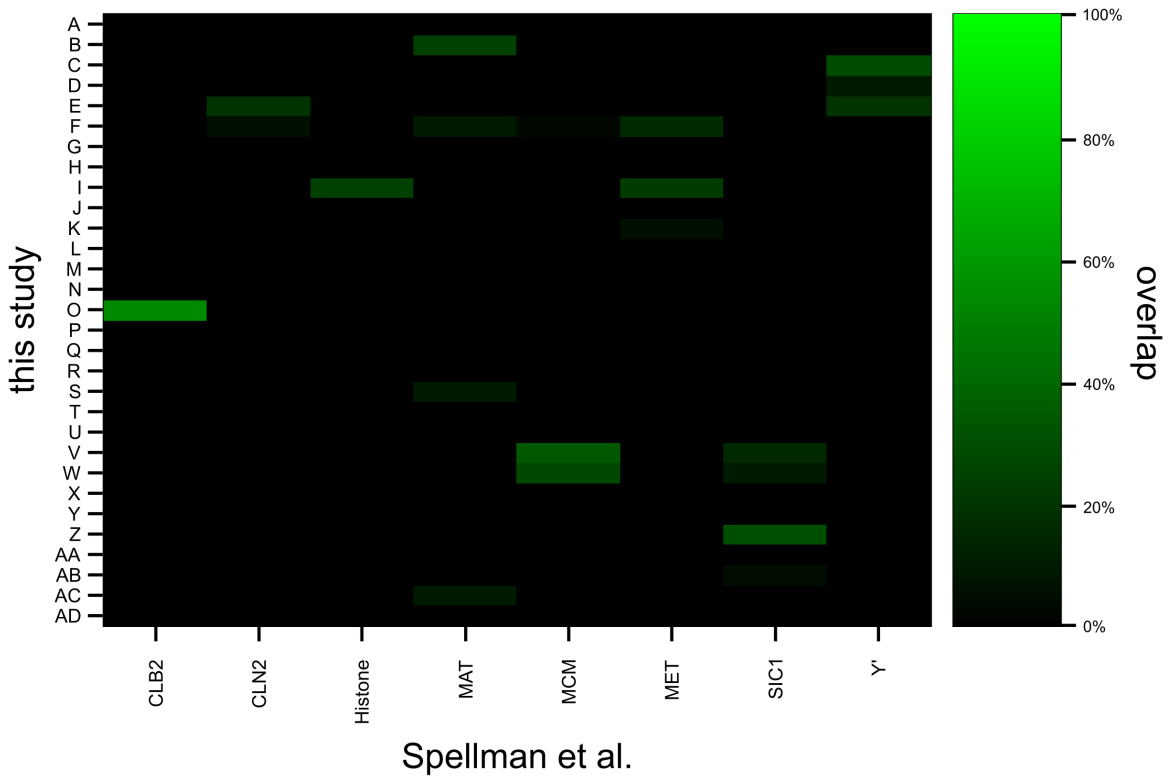

Figure S6 | **Comparisons of gene cluster assignment between wild-type clusters and the clusters from Spellman et al.**[2] The overlap in genes assigned to 30 wild-type clusters (Fig. 3a) to the 8 clusters identified in Spellman et al. (Figures 3,4,6 in ref. 2) are shown. The overlap percentage between two clusters is calculated as the number of genes assigned to both clusters divided by the size of the smaller cluster.

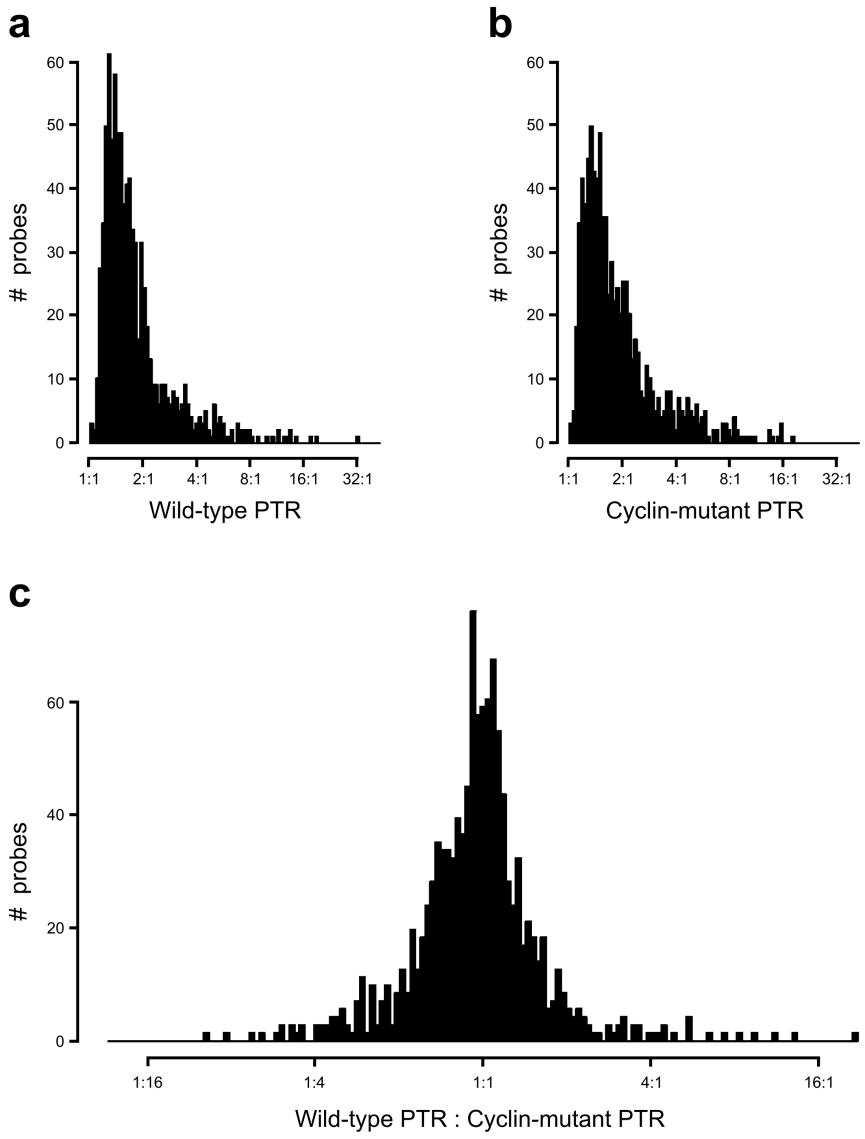

Figure S7 | **Peak to trough ratios for transcripts of periodic genes in wild-type and cyclin-mutant cells.** A histogram of the average peak to trough ratio (PTR) for each of the 882 genes that maintain periodicity in both wild-type and cyclin-mutant cells. PTRs are shown for **a**, wild-type and **b**, cyclin-mutant cells. **c**, Histogram of the ratios of the PTRs of each gene in wild-type vs. cyclin-mutant cells.

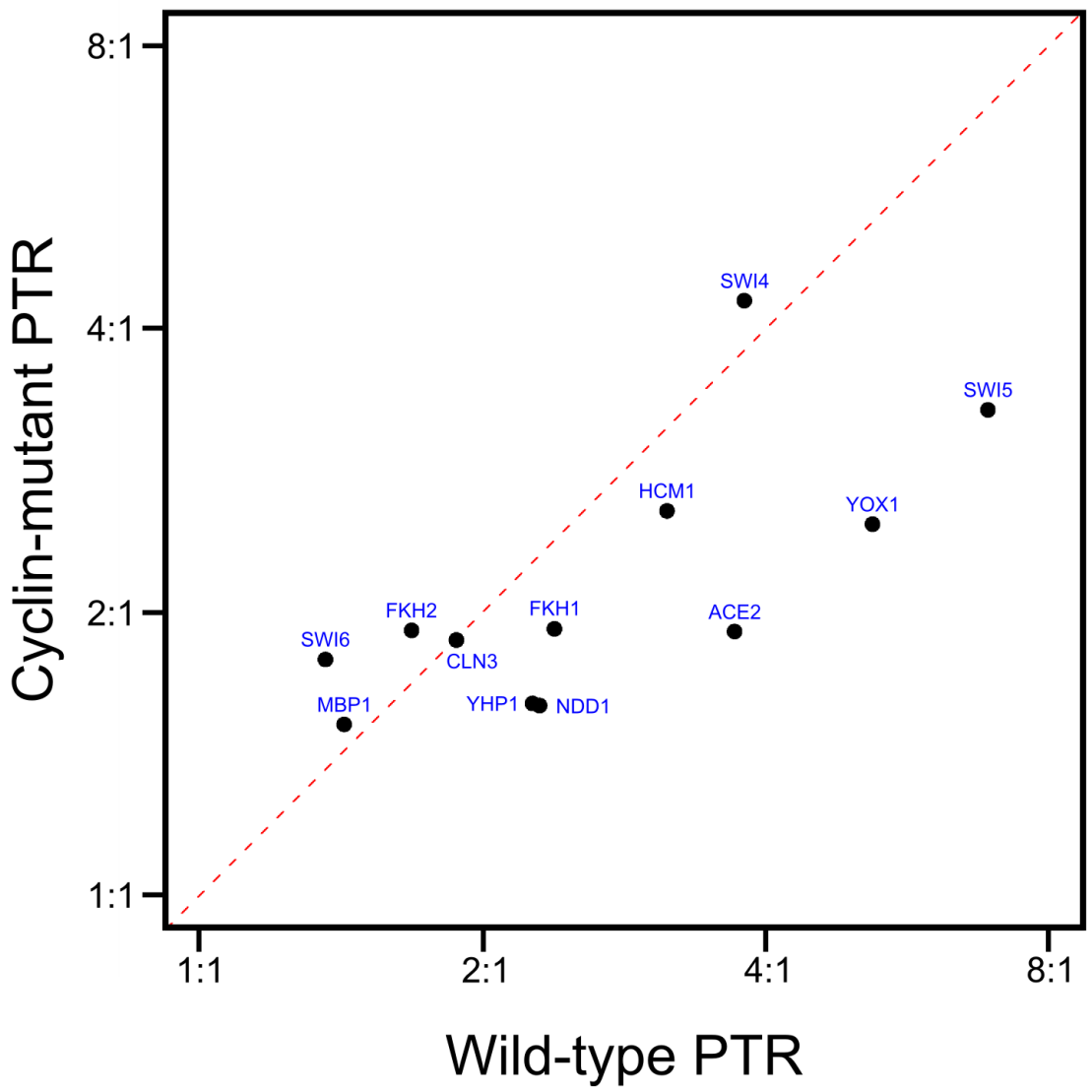

Figure S8 | **Wild-type vs. cyclin-mutant PTRs for transcripts of all transcription factors in the Boolean network model.** The average wild-type PTR (x-axis) plotted against the average cyclin-mutant PTR (y-axis) for each transcription factor (black circle, blue text) in the model depicted in Fig. 4c. The dashed red line is drawn where the ratio between wild-type and cyclin-mutant PTR is one.

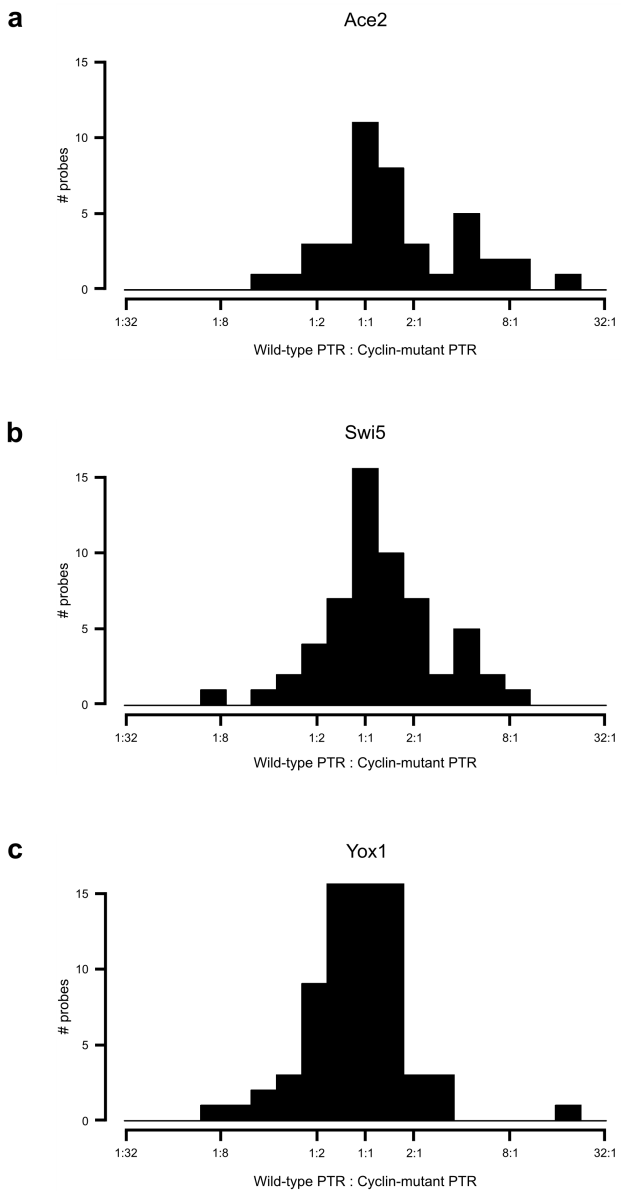

Figure S9 | **Histograms of the ratios of PTRs in wild-type vs. cyclin-mutant cells for the periodic targets of network transcription factors that exhibit reduced expression in cyclin-mutant cells.** Histograms of the ratio between the wild-type and cyclin-mutant PTRs for all genes which were identified as periodic by this study, and are documented targets of **a**, Ace2, **b**, Swi5, and **c**, Yox1 according to the YEASTRACT database.[4]

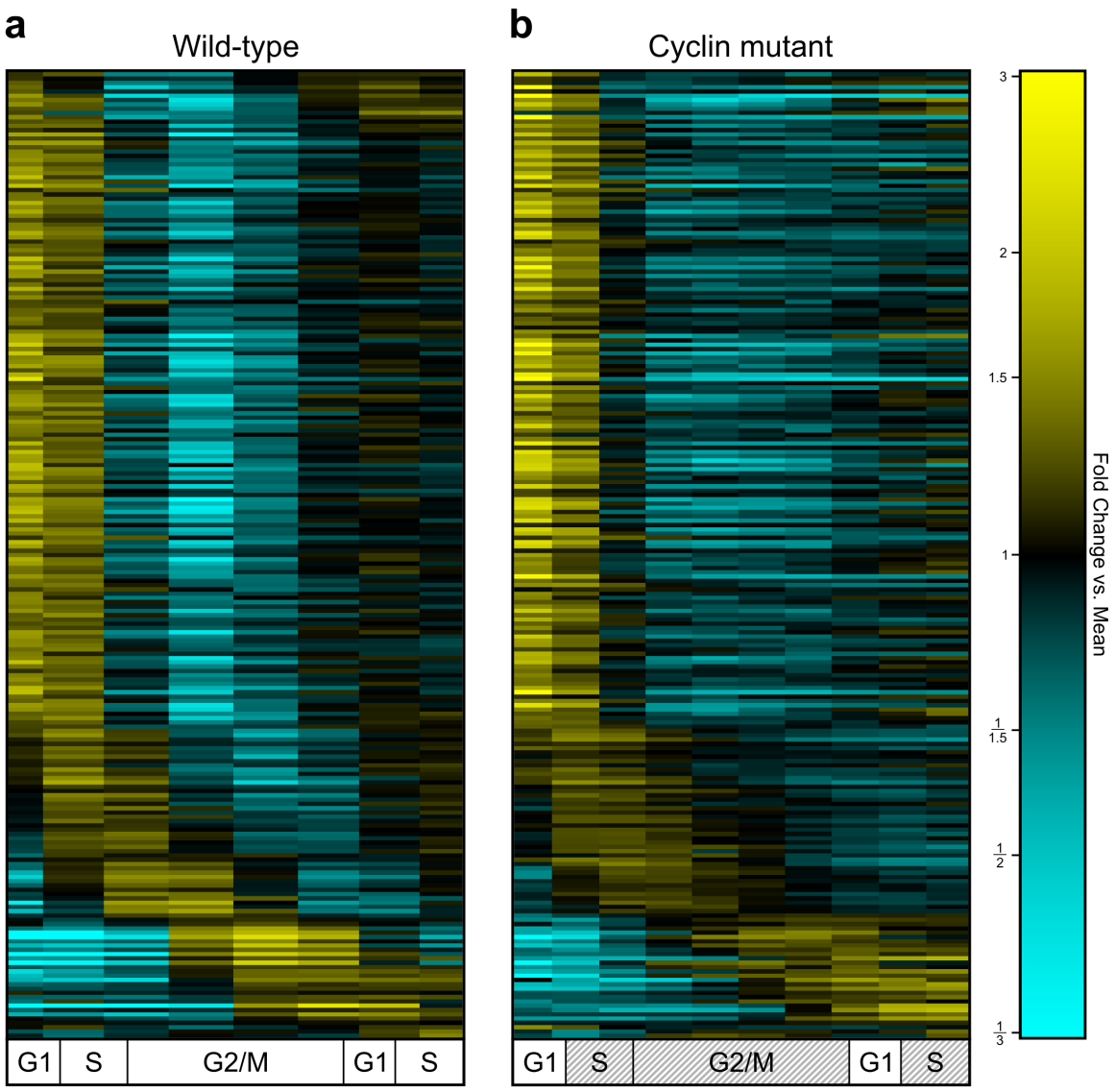

Figure S10 | **Cell cycle dynamics of transcripts for those genes in the consensus periodic set (WTCON) that maintain periodic expression in cyclin-mutant cells.** Heatmaps depicting mRNA levels are shown for **a**, wild-type and **b**, cyclin-mutant cells. Each row in (**a**) and (**b**) represents data for the same gene (ordered gene names are listed in Supplementary Table 2). Transcript levels are depicted and mapped onto a cell-cycle timeline as shown in Supplementary Fig. 3.

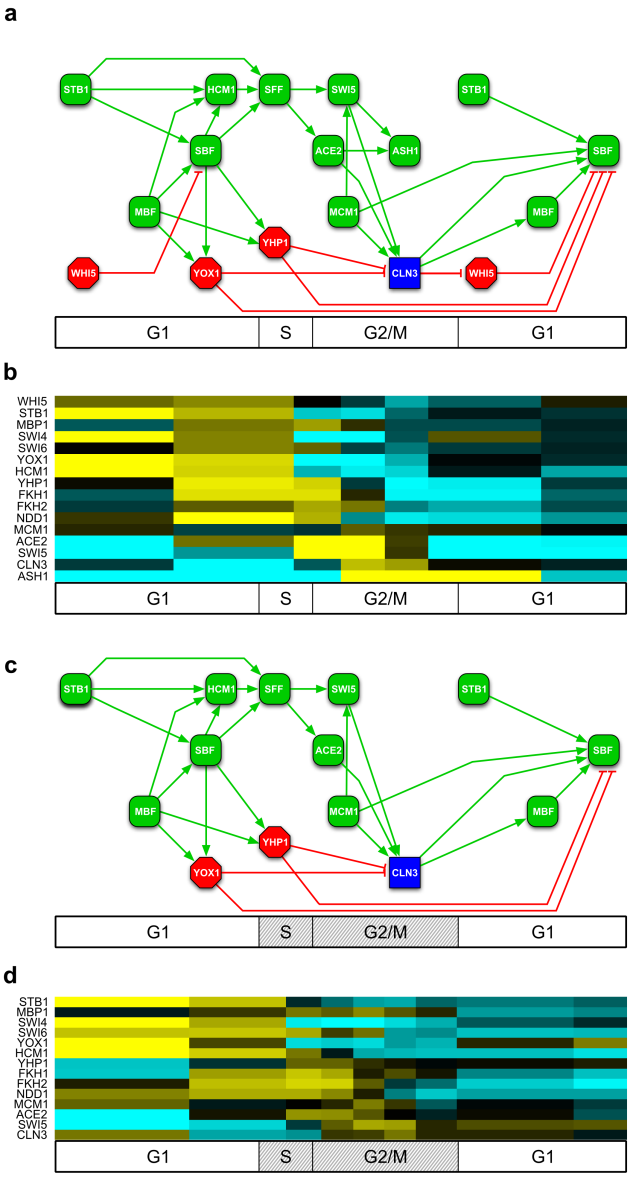

Figure S11 | **Full transcription factor network diagrams for wild-type and cyclin-mutant cells.** Network diagrams (**a**,**c**) are similar to timeline representations of the circular diagram in Fig. 4c. Periodically expressed transcription factors are placed on the cell-cycle timeline on the basis of the time of peak transcript levels in our data sets. Arrows indicate a documented interaction between a transcription factor and promoter elements upstream of a gene encoding another transcription factor (see Supplementary Table 5).[1,4–21] Transcriptional activators are depicted in green, repressors in red, and the cyclin Cln3 in blue. The actual **b**, wild-type and **d**, cyclin-mutant expression of the transcription factors in the networks are shown. Transcript levels are depicted as in Fig. 1. The scale of the cell-cycle timeline has been altered to accommodate multiple G1 events.

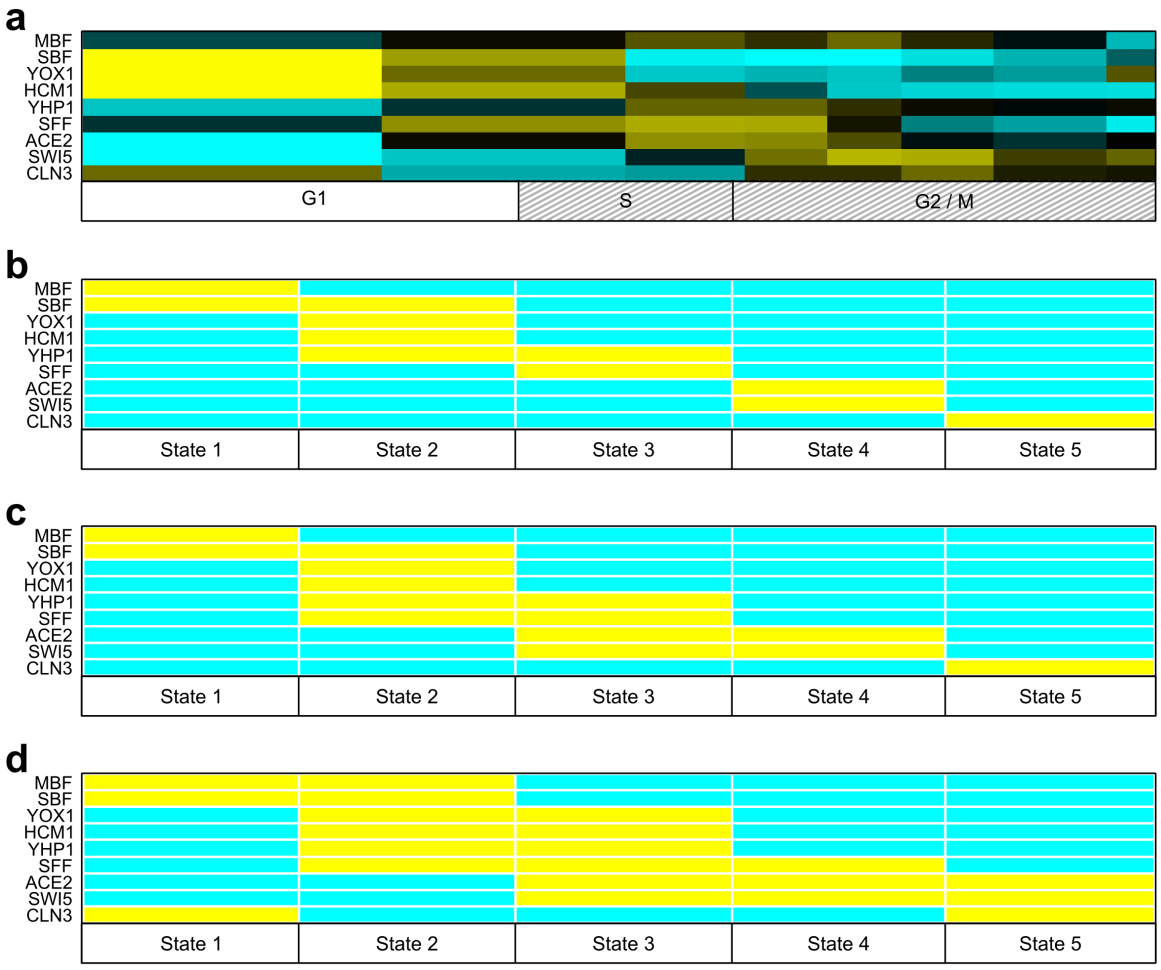

Figure S12 | **A synchronously updating Boolean model can reproduce the sequential order of transcription factor expression.** **a**, The actual expression of the variables in Fig. 4c (with MBP1, SWI4, and FKH2 as proxies for SBF, MBF, and SFF, respectively), as compared to the on/off (yellow/cyan) states of those variables in **b**, Cycle 1, **c**, Cycle 2, and **d**, Cycle 3 (Supplementary Table 6c-e). Transcript levels are depicted as in Fig. 1. The scale of the cell-cycle timeline has been altered to accommodate multiple G1 events.

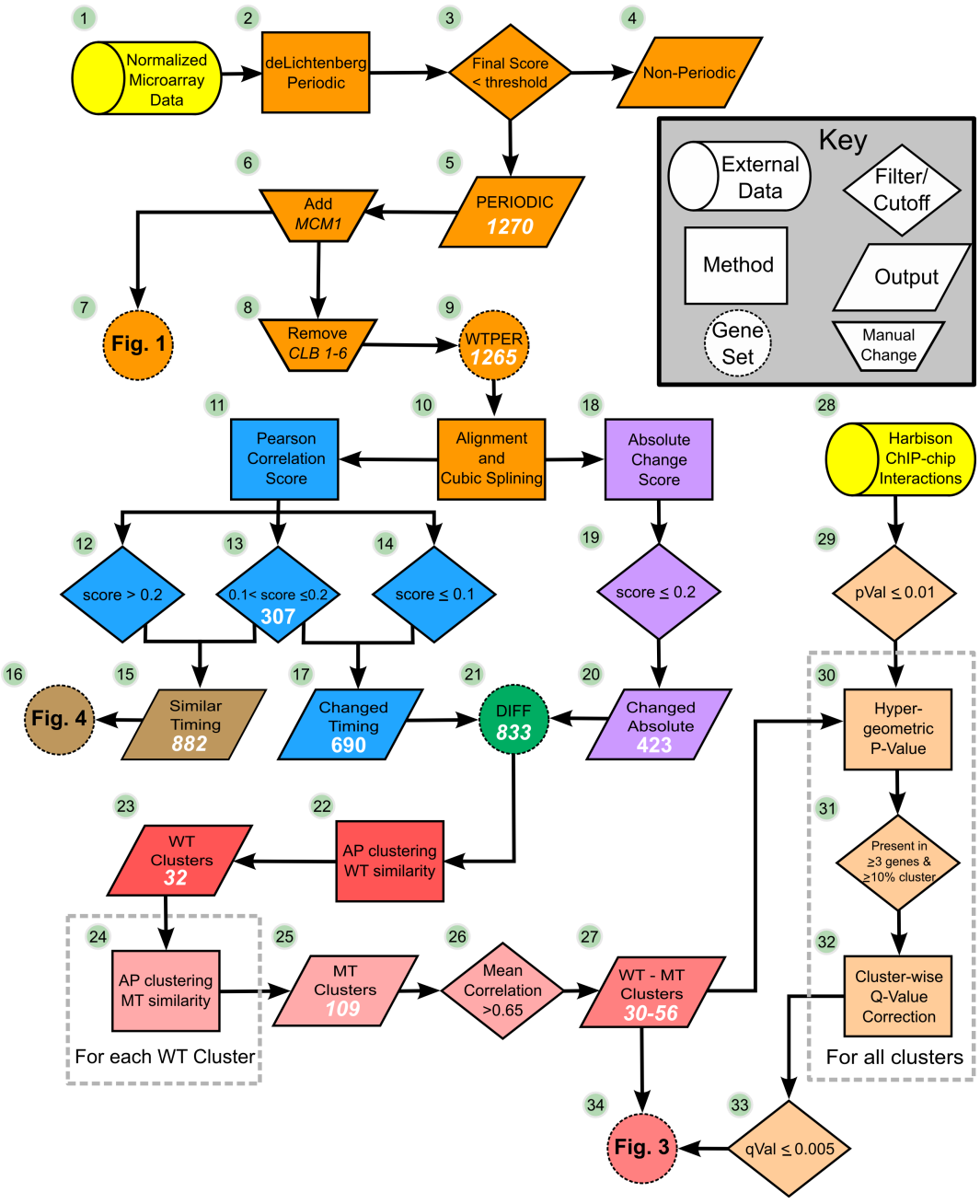

Figure S13 | A schematic of the computational analysis pipeline used in the manuscript. Colors correspond to different analysis topics (e.g., yellow represents identification of periodic genes). Shapes correspond to particular types of procedures or data (e.g., diamonds are filters and cylinders are external data). White numbers within a shape indicate the size of the corresponding gene set (e.g., the 882 in Item 15 indicates that 882 genes maintain their periodic expression in cyclin-mutant cells).

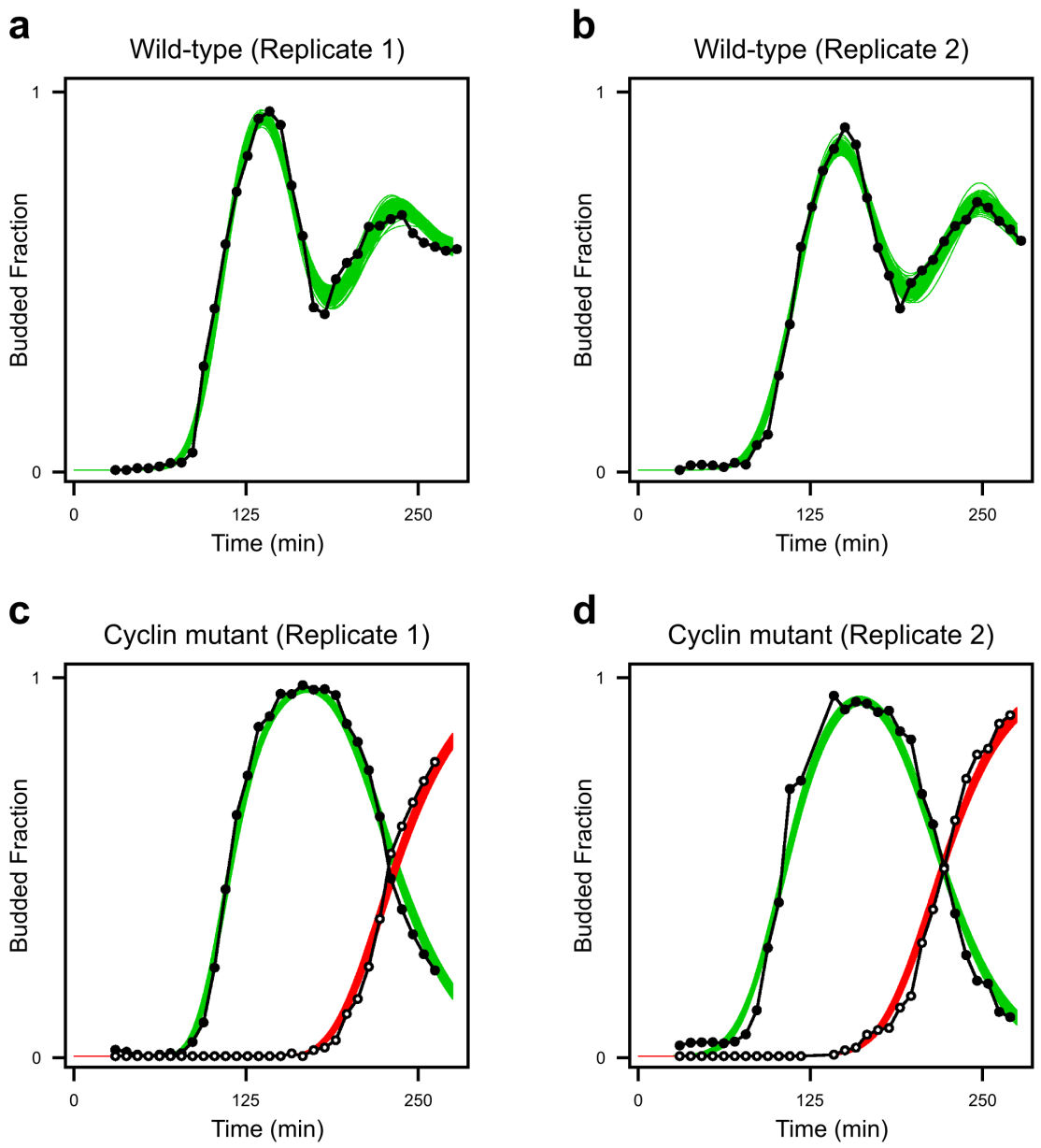

Figure S14 | **CLOCCS model fits for the four time courses.**[3] Fraction of cells with a single bud (black lines, filled circles) and two or more buds (black lines, open circles) for (**a**,**b**), wild-type cells and (**c**,**d**), cyclin-mutant cells. One hundred random realizations from the Markov chain used to fit each experiment were used as parameterizations for the model, and the resulting predicted budding curves for one bud (green lines) and two or more buds (red lines) are shown. The width of the band reflects the degree of posterior uncertainty in the budding curve and can be interpreted as forming a confidence band for the curve on the basis of the uncertainty in the parameters. Parameter estimates for each experiment are given in Supplementary Table 7.

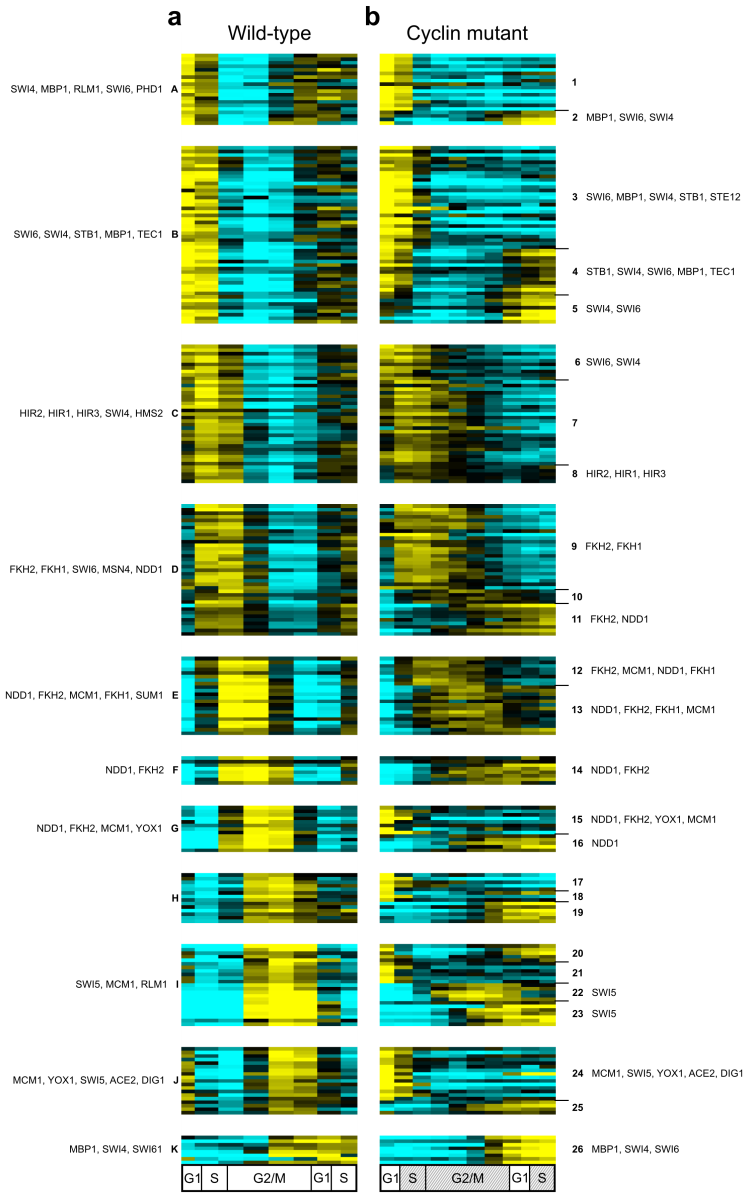

Figure S15 | **Genes in the consensus periodic set (WTCON) exhibiting altered behaviors in the cyclin mutant.** **a**, Clusters of genes with similar expression patterns in wild-type cells. **b**, Subclusters of genes with similarly altered expression patterns in cyclin-mutant cells. Each row in (**a**) and (**b**) represents data for the same gene (gene names are listed in Supplementary Table 2). Transcript levels are depicted and mapped onto a cell-cycle timeline as shown in Fig. 1. Up to five over-represented transcription factors for each cluster are shown (see Section 9). The complete list of over-represented transcription factors are listed in Supplementary Table 8.

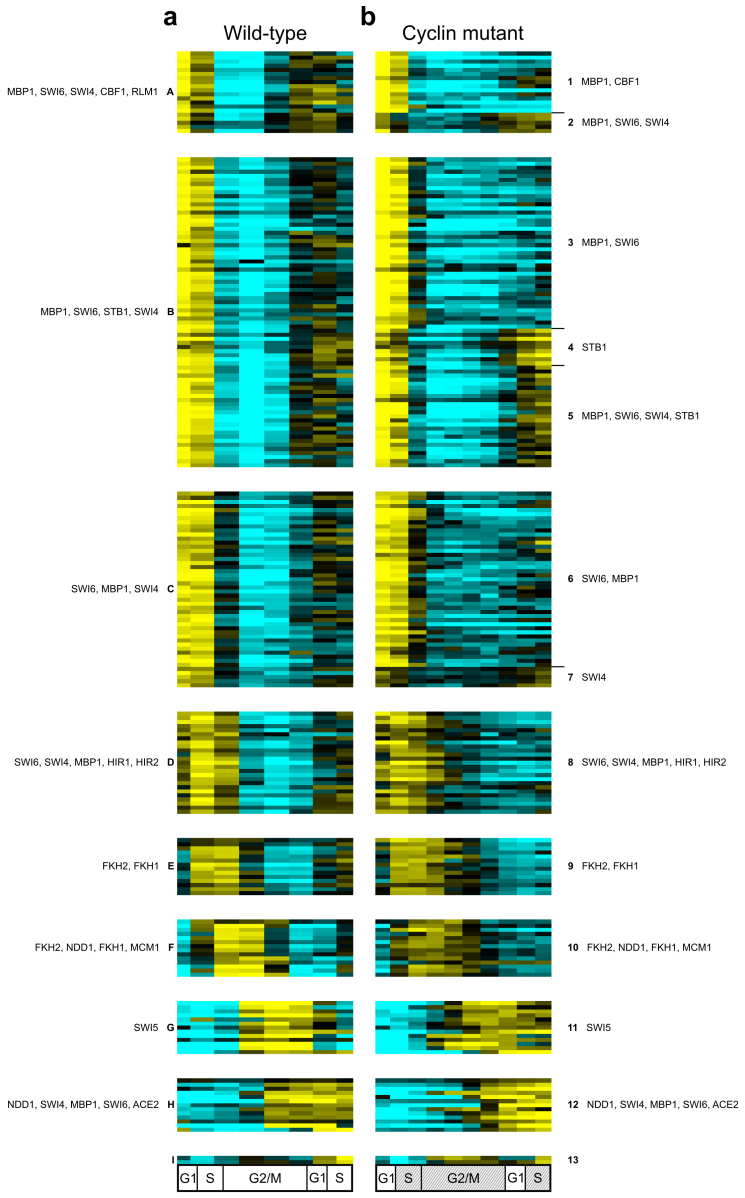

Figure S17 | **Genes in the consensus periodic set (WTCON) maintaining periodicity in the cyclin-mutant cells.** **a**, Clusters of genes with similar expression patterns in wild-type cells. **b**, Subclusters of genes with similar expression patterns within in cyclin-mutant cells. Each row in (**a**) and (**b**) represents data for the same gene (gene names are listed in Supplementary Table 2). Transcript levels are depicted and mapped onto a cell-cycle timeline as shown in Fig. 1. Up to five over-represented transcription factors for each cluster are shown (see Section 9). The complete list of over-represented transcription factors are listed in Supplementary Table 9.

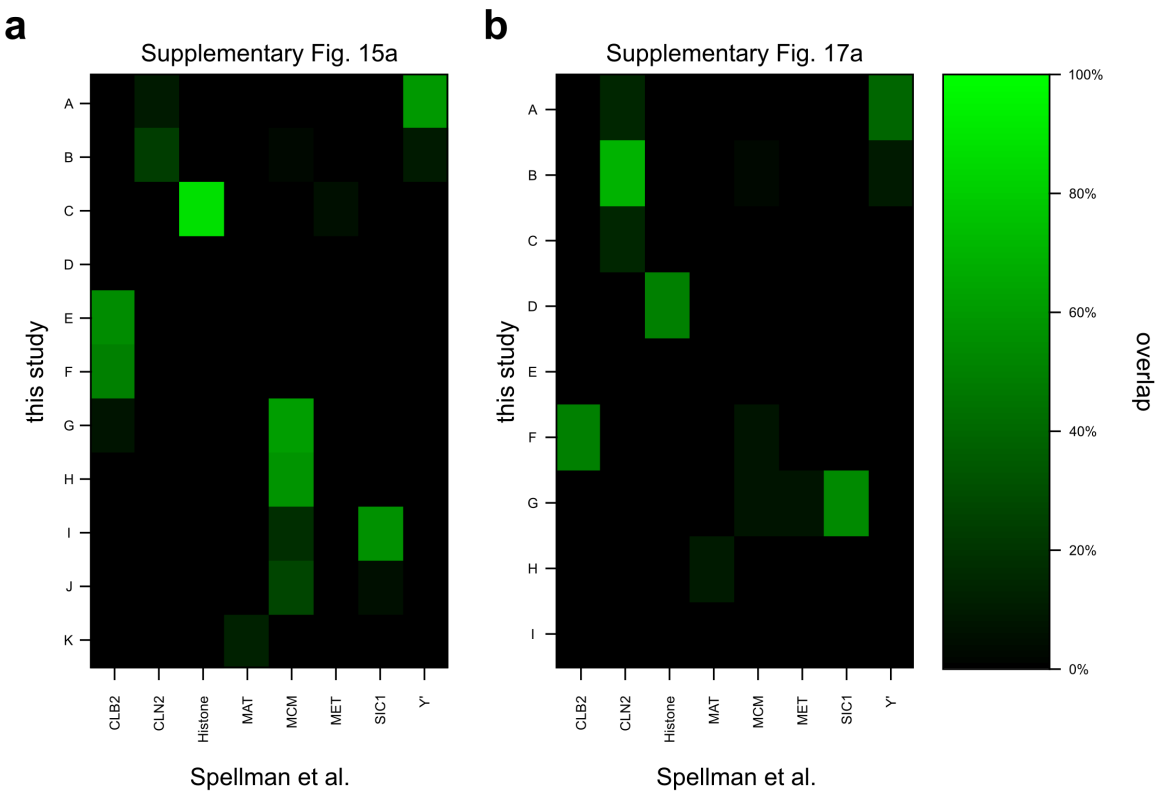

Figure S19 | **Comparisons of gene cluster assignment between wild-type clusters of Supplementary Figs. 15 and 18, and the clusters from Spellman et al.[2]** The overlap in genes assigned to **a**, 11 (Supplementary Fig. 15a) and **b**, 9 (Supplementary Fig. 17a) wild-type clusters to the 8 clusters identified in Spellman et al. (Figures 3,4,6 in ref. 2) are shown. The overlap percentage between clusters is calculated as shown in Supplementary Fig. 6.

Supplemental Information to accompany "Global control of cell-cycle transcription by coupled CDK and network oscillators"

by David A. Orlando, Charles Y. Lin, Allister Bernard, Jean Y. Wang, Joshua E.S. Socolar, Edwin S. Iversen, Alexander J. Hartemink, and Steven B. Haase

Our complete data analysis pipeline is depicted schematically in Supplementary Fig. 13. For increased clarity of presentation, the following sections periodically refer to the numbered items in Supplementary Fig. 13 as appropriate.

1 Data normalization (Item 1)

CEL files from all 60 Affymetrix Yeast 2.0 oligonucleotide arrays were normalized and summarized using the dChip[22] method as implemented by the `affy` package (v. 1.8.1) in Bioconductor,[23] a software suite for analysis of functional genomics data within the R statistical programming environment.[24] The command we used was `expresso(inputdata, normalize.method="invariantset", bg.correct=FALSE, pmcorrect.method="pmonly", summary.method="liwong")`. The output of this command provides a measure of the absolute transcript level for each probe in arbitrary units. Only probes mapping to *Saccharomyces cerevisiae* genes were retained, and normalized transcript levels for these genes are indicated as Item 1 in Supplementary Fig. 13.

2 Identifying periodic genes (Items 2-9)

Genes exhibiting periodic behavior were determined using the method of de Lichtenberg and colleagues.[25] Wild-type data from both replicates—with the CLOCCS[3] recovery phase (Gr) removed—were used as input. Permutation p-values assessing 'degree of regulation' and 'degree of periodicity' were calculated for each gene in each wild-type replicate (one million permutations were used for each). Following de Lichtenberg, these four p-values (two from each replicate) were normalized and combined into a final score for each gene. We chose to identify periodic genes by defining a threshold on the basis of the final de Lichtenberg score rather than on the basis of rank. A gene with all four p-values of 0.2 would be given a final score of 26,020,272, and we used this as our score threshold. This threshold resulted in a total of 1270 genes being labeled as periodic. The gene MCM1 was not in this list, but because of its documented role in regulating cell-cycle transcription[15] and its periodic expression by visual inspection, it was added to the list, resulting in the 1271 periodic wild-type genes shown in Fig. 1. The position of each gene in the figure, as well

as its periodicity rank, is given in Supplementary Table 1. Because the remainder of our analysis entails comparison between wild-type and cyclin-mutant cells, we removed the six B-cyclin genes from the set of 1271 since their behavior was altered by gene disruption. We refer to the resultant set of 1265 genes as Wild Type PERiodic (WTPER, Item 9).

3 Comparison of periodic genes to previously identified periodic gene lists

We compared the overlap between the set of 1271 periodic genes identified in this study to the sets of 991 and 800 periodic genes identified in the Pramila et al.[1] and Spellman et al.[2] studies, respectively (Supplementary Fig. 2). There was only partial overlap between the sets, with our set containing 58% and 64% of the genes identified by Pramila et al. and Spellman et al., respectively (Spellman et al. and Pramila et al. overlap by 73%). The exact reasons for these incomplete overlaps are unknown, but could be the result of differences in the array platforms (*in situ* oligonucleotide vs. spotted cDNA), synchronization techniques (elutration vs. α-factor or *cdc* mutants), and algorithms used for periodic gene identification.

We have examined the set of 440 genes identified as periodic by all three studies, referred to as Wild Type CONensus (WTCON, Supplementary Fig. 3 and Supplementary Table 2). Interestingly the overlap appears to reflect the genes which exhibit a relatively high dynamic range of expression (Supplementary Fig. 4b, Row 2 vs. Row 3). We have repeated many of the analyses performed on the more comprehensive WTPER gene set on the smaller set of consensus periodic genes in WTCON. Results of those analyses are detailed in the sections below.

4 Calculation of peak to trough ratios

The dynamic range of transcription for any gene can be measured by examining the ratio of the peak transcript level to the trough. Peak to trough ratios (PTRs) for Supplementary Tables 1-3 and Supplementary Figs. 4, 7, 8, and 9, were calculated as the maximum expression value in a given window divided by the minimum expression value in that window. The window examined covered expression from the first G1 to the end of the second S phase. The wild-type and cyclin-mutant PTRs reported are the average PTRs calculated in the respective replicates for each dataset.

5 CLOCCS model fitting

To accurately compare cell-cycle gene expression profiles across our two wild-type and two cyclin-mutant datasets, we used the CLOCCS model[3] to correct for timing differences inherent in synchrony/time-series experiments, and for the modest differences in the cell-cycle time between wild-type and cyclin-mutant cells. The previously published CLOCCS model accurately predicts the cell-cycle position and distribution of synchronized cell populations at each point in a time series for wild-type yeast populations. Only minor modifications to the model are required to predict cell-cycle position and distribution of cyclin-mutant populations.

In terms of modeling, the most important difference between wild-type and cyclin-mutant populations is that cyclin-mutant cells do not divide and hence no new daughter cell cohorts can arise. The CLOCCS model for cyclin-mutant cells thus ignores cohorts other than the initial $\{G = 0, R = 0\}$ cohort. As a result, the mother/daughter offset parameter δ is no longer used because it relates only to the effects of asymmetric cell division. The modified CLOCCS model for cyclin-mutant cells is:

$$\begin{aligned} \Pr(P_t|\Theta,t) &= \sum_G \sum_R \Pr(P_t|\Theta,G,R,t)\Pr(G|\Theta,R,t)\Pr(R|\Theta,t) && (1)\\ &= \Pr(P_t|\Theta,G=0,R=0,t) && (2)\\ &= \phi\left(\frac{P_t-(-\mu_0+t)}{\sqrt{\sigma_0^2+t^2\cdot\sigma_v^2}}\right) && (3) \end{aligned}$$

where $\phi(\cdot)$ is the standard normal density function, $\Theta = \sigma_0^2, \sigma_v^2, \mu_0, \lambda, \beta$, and all variables are defined exactly as in the original CLOCCS model.[3]

Unlike in a wild-type population where cells are either budded or unbudded, cyclin-mutant cells never lose their first bud, but grow an additional bud at the G1/S border of each subsequent cell cycle. Hence, before their first S phase ($P_t < \lambda\beta$), cyclin-mutant cells will have no buds, between their first and second S phases ($\lambda\beta \le P_t < \lambda(1+\beta)$), they will have one bud, between their second and third S phases ($\lambda(1+\beta) \le P_t < \lambda(2+\beta)$), they will have two buds, and so on. We use this to calculate the expected percentages of cells with j buds at time t:

$$\pi_{jt} = \begin{cases} \Phi\left(\frac{\lambda(j+\beta)-(-\mu_0+t)}{\sqrt{\sigma_0^2+t^2\cdot\sigma_v^2}}\right) - \Phi\left(\frac{\lambda(j-1+\beta)-(-\mu_0+t)}{\sqrt{\sigma_0^2+t^2\cdot\sigma_v^2}}\right) & \text{if } j \ge 1 \\ \Phi\left(\frac{\lambda\beta-(-\mu_0+t)}{\sqrt{\sigma_0^2+t^2\cdot\sigma_v^2}}\right) & \text{if } j = 0 \end{cases}$$

where $\Phi(\cdot)$ is the standard normal cumulative density function. We can estimate the parameters Θ of the modified CLOCCS model by maximizing the multinomial likelihood function:

$$L(\Theta) \propto \prod_{t=1}^{T}\prod_{j=0}^{\infty} \pi_{jt}^{c_{jt}}$$

where $c_{jt} = \sum_i X_{ijt}$ is the count of the number of cells with j buds at time t, and T is the number of timepoints at which budded cells are counted.

The CLOCCS model was fit on wild-type datasets using 32 timepoints of budding index data measured every 8 minutes, starting 30 minutes after release (Supplementary Fig. 14a and b). Similarly, the modified CLOCCS model was fit on cyclin-mutant datasets using 30 timepoints in one replicate (Supplementary Fig. 14c) and 29 timepoints in the other (Supplementary Fig. 14d) of budding index data measured every 8 minutes, starting 30 minutes after release. When fitting the cyclin-mutant datasets, since β and μ_0 are not simultaneously identifiable from the cyclin-mutant budding index data, β was fixed to be 0.15. CLOCCS parameter estimates are given in Supplementary Table 7.

6 Data alignment and cubic splining (Item 10)

Further analysis steps involve comparison of gene expression profiles across different experiments, and alignment is imperative so that comparisons are made on the basis of cell-cycle position rather than clock time. Having the CLOCCS parameter estimates described above enables the alignment of datasets onto a common cell-cycle lifeline. We used a procedure similar to that described in Orlando et al.[3] to align all four of our datasets such that the observed measurements were aligned at the boundaries between G1, S, and G2/M. When performing statistical comparisons of these aligned expression profiles, we fit each expression profile with a cubic spline and then sampled at 1000 equally spaced points from the start of the first G1 to the end of the second S phase.

7 Identifying genes whose expression changes in cyclin-mutant cells (Items 11-21)

To determine if a gene changes its expression pattern in cyclin-mutant cells, we developed two scores: a Pearson correlation score (PCS) and an absolute change score (ACS). The PCS detects changes in timing of expression, but is relatively insensitive to changes in amplitude. The ACS is more sensitive to changes in amplitude of expression.

Each score is computed on the basis of two statistics, WTMT and MTMT. The exact form of these statistics for each score ($WTMT_P$ and $MTMT_P$ for PCS; $WTMT_A$ and $MTMT_A$ for ACS) is given in the subsections below. The WTMT statistics capture change in gene expression from wild-type to cyclin-mutant cells, while the MTMT statistics capture variability in gene expression between

cyclin-mutant replicates. As such, the MTMT statistics for all genes comprise a background distribution against which WTMT statistics can be compared. Scores for the change in expression for gene i relative to the corresponding background distribution are computed in each case by calculating the fraction of MTMT statistics that are more extreme (lower in the case of PCS and higher in the case of ACS) than the WTMT statistic for gene i. Thus for gene i the PCS is calculated as the fraction of all MTMT_P statistics lower than WTMT_P^i, and the ACS is calculated as the fraction of all MTMT_A statistics greater than WTMT_A^i. A gene is called different if either of the scores is less than or equal to 0.2 (when analyzing WTPER, a PCS equal to 0.2 roughly corresponds to Pearson correlation of 0.75). This cutoff resulted in a set of 833 genes that are called different between wild-type and cyclin-mutant cells (denoted DIFF, Item 21).

We also took advantage of the amplitude insensitivity of the PCS to select genes that, although they may change in amplitude, do not change in timing of expression and thus can be said to retain their periodicity. A gene is called similar if its PCS was greater than 0.1 (roughly corresponding to a Pearson correlation of 0.5 given WTPER) . This cutoff resulted in a set of 882 genes (Item 15) that retain their periodicity between wild-type and cyclin-mutant cells (Fig. 4). The calculated scores for each gene in WTPER can be found in Supplementary Table 1.

We performed a similar analysis on the set of 440 genes identified as periodic by our study and two previous studies (WTCON, see Section 3).[1,2] Repeating the above analysis required re-computing the ACS and PCS scores for each gene because the background distribution from which they were calculated changed when the input gene set changed. We found that even among the WTCON gene set, greater than 50% still displayed periodic behaviors in cyclin-mutant cells, with genes being transcribed throughout the cell cycle (Supplementary Fig. 10). We identified 307 genes as changing from wild-type to cyclin-mutant cells, and 225 were identified as retaining their periodicity (scores calculated for WTCON can be found in Supplementary Table 2). The findings for WTCON, a very restrictive set of periodic genes with relatively large dynamic ranges of expression, are consistent with the results from the more comprehensive set of periodic genes, WTPER.

7.1 Pearson correlation statistics (Item 11)

Let w_i^1 and w_i^2 represent the splined wild-type expression profiles for gene i in wild-type replicates 1 and 2, respectively. Similarly, let m_i^1 and m_i^2 represent the splined cyclin-mutant expression profiles for gene i in cyclin-mutant replicates 1 and 2, respectively. The WTMT Pearson correlation statistic for gene i is defined as:

$$\text{WTMT}_\text{P} = \max(\rho(w_i^1, m_i^1), \rho(w_i^1, m_i^2), \rho(w_i^2, m_i^1), \rho(w_i^2, m_i^2))$$

and the MTMT Pearson correlation statistic for gene i is defined as:

$$\mathsf{MTMT_P} = \rho(m_i^1, m_i^2)$$

where $\rho(f, g)$ is the Pearson correlation between f and g.

7.2 Absolute change statistics (Item 18)

The WTMT absolute change statistic for gene i is defined as:

$$\mathsf{WTMT_A} = \min(\tau(w_i^1, m_i^1), \tau(w_i^1, m_i^2), \tau(w_i^2, m_i^1), \tau(w_i^2, m_i^2))$$

and the MTMT absolute change statistic for gene i is defined as:

$$\mathsf{MTMT_A} = \tau(m_i^1, m_i^2)$$

where $\tau(f, g) = \frac{||f-g||_1}{\frac{1}{2}||f+g||_1}$.

8 Clustering to characterize expression changes in cyclin-mutant cells (Items 22-27)

To further characterize how transcription changes in response to the loss of B-cyclins, we performed a two-step clustering of the 883 genes in DIFF (Item 21). Both clustering steps use the affinity propagation algorithm of Frey and Dueck.[26] The first step (Item 22) clustered the 883 genes using only their wild-type expression profiles, defining the similarity between genes i and j as:

$$\frac{\rho(w_i^1, w_j^1) + \rho(w_i^2, w_j^2)}{2} - 1$$

with S_{kk} set to the value of -1 for all k. This first round of clustering produced 32 wild-type clusters. Each wild-type cluster was then subclustered in a second round of clustering (Item 24) based only on cyclin-mutant expression profiles, defining the similarity between genes i and j as:

$$\frac{\rho(m_i^1, m_j^1) + \rho(m_i^2, m_j^2)}{2} - 1$$

with S_{kk} again set to the value of -1 for all k. This second round of clustering produced a total of 109 subclusters within the 32 wild-type clusters. To ensure that subclusters had a sufficiently coherent expression pattern, subclusters whose average Pearson correlation of cyclin-mutant expression was less than 0.65 were removed (Item 26). Fifty three subclusters—including all the subclusters of two wild-type clusters—were removed by this filter, resulting in a final set of 513

genes clustered into 30 wild-type clusters and 56 cyclin-mutant subclusters (Fig. 3 and Supplementary Fig. 5). These resulting clusters have a high average Pearson correlation (within cluster) of 0.808 and 0.790 for wild-type clusters and cyclin-mutant subclusters, respectively (Supplementary Table 3) suggesting a high degree of co-regulation within each cluster.

9 Identifying over-represented transcription factors (Items 28-34)

The 30 wild-type clusters exhibit coherent wild-type expression patterns, and the 56 cyclin-mutant subclusters exhibit both coherent wild-type and cyclin-mutant expression patterns. If these coherent expression patterns are regulated by common transcription factors (TFs), we may expect to find certain TFs significantly associated with each cluster or subcluster. We tested this hypothesis by looking for over-represented TF binding to promoters of genes within each cluster and subcluster using the ChIP-chip data of Harbison et al.[7] This dataset provides p-values for a total of 206 TFs binding to the intergenic (promoter) regions of most genes in *S. cerevisiae*. We chose all p-values less than or equal to 0.01 as evidence of a binding interaction between a TF and an intergenic region. We identified clusters or subclusters enriched for the given set of 206 TFs using a hypergeometric test (Item 30). To increase the likelihood that the TF/cluster pairs we identified are biologically (and not just statistically) significant, we removed TFs that bound less than 3, or less than 10% of the genes in a cluster or subcluster (Item 31). To correct for multiple hypothesis testing (since more than one TF could be enriched for a cluster or subcluster), we used the q-value method of Storey[27] to calculate q-values that act as FDR-corrected enrichment scores for each TF for every cluster and subcluster. A TF was designated as being over-represented in a given cluster or subcluster if its q-value was less than or equal to 0.005 (Item 33). The expression heatmaps, centroid line graphs, and over-represented TFs for all clusters and subclusters can be found in Fig. 3, Supplementary Fig. 5, and Supplementary Table 4.

10 Clustering to characterize expression and identify over-represented transcription factors within the WTCON gene set

We repeated the analysis presented in Sections 8 and 9 twice more; once using the WTCON set of genes identified as different, and once using the WTCON genes identified as maintaining their periodicity. These two analyses provide a relatively complete description of the high-confidence periodic genes in WTCON that are coordinately regulated in wild-type and cyclin-mutant cells. The clustering analysis of the 307 WTCON genes identified as different (Supplementary Table 2) resulted in 11 wild-type clusters and 26 cyclin-mutant subclusters (Supplementary Fig. 15 and

Supplementary Fig. 16), with an average Pearson correlation (within cluster) of 0.880 and 0.817, respectively (Supplementary Table 3). The clustering analysis of the 225 WTCON genes which retain their periodicity resulted in 9 wild-type clusters and 13 cyclin-mutant subclusters (Supplementary Fig. 17 and Supplementary Fig. 18), with an average Pearson correlation (within cluster) of 0.874 and 0.832, respectively (Supplementary Table 3). The overlap between the wild-type clusters from both clusterings to those identified by Spellman et al.[2] is available in Supplementary Fig. 19. We also identified over-represented transcription factors in each cluster and subcluster (see Section 9). Up to the top 5 over-represented transcription factors for each cluster and subcluster are shown in Supplementary Fig. 15 and Supplementary Fig. 17, with the complete lists available in Supplementary Table 8 and Supplementary Table 9.

11 Identifying a transcriptional network

We constructed transcriptional networks using the set of periodically expressed TFs for wild-type cells and the subset of those which maintained periodic expression for cyclin-mutant cells. The set of all TF genes was defined by taking the union of all genes profiled by Harbison et al.[7] or listed as TFs in the YEASTRACT database.[4] In addition to this set, we added MBP1, WHI5, and CLN3. Mbp1 is a TF that exhibited periodic behavior, albeit below our periodicity score threshold, which along with Swi6 forms the MBF complex that is known to regulate G1 transcription.[28] Whi5 is a repressor of MBF and SBF transcription factor complexes,[20,21] and Cln3 is known to directly inhibit Whi5 and thereby activate MBF and SBF complexes.[20,21] While the genes encoding most transcription factors in the network are transcribed at normal levels in cyclin-mutant cells, some (*ACE2*, *SWI5*, and *YOX1*) are expressed at reduced levels (Fig. 2f and Supplementary Fig. 8). However, the fact that their target genes (e.g., the Ace2 targets *SIC1* and *NIS1*; see Fig. 2c and d, and Supplementary Fig. 9) are expressed at near-normal levels indicates that the periodic expression of these transcription factors is still biologically relevant.

A node corresponding to each TF was placed on the cell-cycle lifeline according to its time of peak expression (temporal ordering of nodes is preserved, but the scale within G1 is expanded to accommodate the depiction of multiple G1 events). Edges between nodes corresponding to TF-promoter interactions were drawn if the ChIP-chip data of Harbison et al.[7] reported a p-value less than or equal to 0.01 or if the interaction had been documented in the literature.[1,4–21] Edges were classified as either activating (green) or repressing (red) on the basis of the function of the TF (those TFs whose function was ambiguous (e.g., RAP1) were pruned from the network). Self-activating edges and activating edges whose length was more than 40% of the length of the cell cycle were pruned. Nodes that had neither input nor output edges were pruned. TFs that act

in known complexes (MBF, SBF, and SFF, reviewed in Wittenberg et al.[29]) were collapsed into a single node. The cyclin-mutant network was constructed using the same procedure, but TFs that did not maintain their timing in cyclin-mutant cells were excluded. The resulting wild-type and cyclin-mutant networks are shown in Supplementary Fig. 11a and c.

12 Boolean model construction

A synchronously updating Boolean model was constructed for all TFs that remained periodic in cyclin-mutant cells. The transcription network architecture was constructed as described above. TFs that did not have both input and output edges with high-confidence literature support were pruned from the network (see Supplementary Fig. 11 for full network diagrams in wild-type and cyclin-mutant cells and Supplementary Table 5 for documentation of literature support). The remaining TFs were treated as variables in our model and the set of controlling Boolean logic functions were determined as the strictest (i.e., AND wherever possible) combinatorial functions over incoming edges that reproduced the observed data (Supplementary Fig. 12). Initial choices of logic functions are shown in Supplementary Table 6a. To examine robustness, we determined the attractors for all possible starting states given these initial choices of logic functions. Results are shown in Supplementary Table 6b, Row 1. We found that 80.3% of all the 512 possible starting states enter a cycle containing five states (Cycle 1). The values of all TFs in each of the five states in Cycle 1 are shown in Supplementary Table 6c.

To determine whether this cyclic attractor was dependent on our initial choice of logic functions (Supplementary Table 6a), we examined models generated with all possible simple logic functions over the activating inputs to the CLN3, SFF, and repressor variables. The repressor variable represents YOX1 and YHP1, and the activating logics determine if these repressors can inhibit their targets only when both components are active (AND logic) or when either component is active (OR logic). For each of the models, we determined the final attractor for all possible starting states (Supplementary Table 6b). This analysis revealed the presence of two additional five-state cycles, Cycle 2 and Cycle 3. Cycle 2 and Cycle 3 (Supplementary Table 6d and e) are qualitatively similar to Cycle 1 (Supplementary Table 6c). These cycles maintain the same temporal order of expression as Cycle 1 (Supplementary Fig. 12b), and differ only in the duration of expression of certain TFs (Supplementary Fig. 12c and d).

References

[1] Pramila, T., Wu, W., Miles, S., Noble, W. & Breeden, L. The Forkhead transcription factor Hcm1 regulates chromosome segregation genes and fills the S-phase gap in the transcriptional circuitry of the cell cycle. *Genes & Development* **20**, 2266–2278 (2006).

[2] Spellman, P. *et al.* Comprehensive identification of cell cycle-regulated genes of the yeast Saccharomyces cerevisiae by microarray hybridization. *Molecular Biology of the Cell* **9**, 3273–3297 (1998).

[3] Orlando, D. *et al.* A probabilistic model for cell cycle distributions in synchrony experiments. *Cell Cycle* **6**, 478–488 (2007).

[4] Teixeira, M. *et al.* The YEASTRACT database: A tool for the analysis of transcription regulatory associations in Saccharomyces cerevisiae. *Nucleic Acids Research* **34**, D3–D5 (2006).

[5] Workman, C. *et al.* A Systems Approach to Mapping DNA Damage Response Pathways. *Science* **312**, 1054–1059 (2006).

[6] Bean, J., Siggia, E. & Cross, F. High Functional Overlap Between MluI Cell-Cycle Box Binding Factor and Swi4/6 Cell-Cycle Box Binding Factor in the G1/S Transcriptional Program in Saccharomyces cerevisiae. *Genetics* **171**, 49–61 (2005).

[7] Harbison, C. *et al.* Transcriptional regulatory code of a eukaryotic genome. *Nature* **431**, 99–104 (2004).

[8] Iyer, V. *et al.* Genomic binding sites of the yeast cell-cycle transcription factors SBF and MBF. *Nature* **409**, 533–8 (2001).

[9] Lee, T. *et al.* Transcriptional Regulatory Networks in Saccharomyces cerevisiae. *Science* **298**, 799–804 (2002).

[10] Horak, C. *et al.* Complex transcriptional circuitry at the G1/S transition in Saccharomyces cerevisiae. *Genes & Development* **16**, 3017–3033 (2002).

[11] Simon, I. *et al.* Serial Regulation of Transcriptional Regulators in the Yeast Cell Cycle. *Cell* **106**, 697–708 (2001).

[12] Zhu, G. *et al.* Two yeast forkhead genes regulate the cell cycle and pseudohyphal growth. *Nature* **406**, 90–4 (2000).

[13] Pic, A. *et al.* The forkhead protein Fkh2 is a component of the yeast cell cycle transcription factor SFF. *The EMBO Journal* **19**, 3750–3761 (2000).

[14] Pic-Taylor, A., Darieva, Z., Morgan, B. & Sharrocks, A. Regulation of cell cycle-specific gene expression through cyclin-dependent kinase-mediated phosphorylation of the forkhead transcription factor Fkh2p. *Mol. Cell. Biol* **24**, 10036–10046 (2004).

[15] Althoefer, H., Schleiffer, A., Wassmann, K., Nordheim, A. & Ammerer, G. Mcm1 is required to coordinate G2-specific transcription in Saccharomyces cerevisiae. *Molecular and Cellular Biology* **15**, 5917–5928 (1995).

[16] Koranda, M., Schleiffer, A., Endler, L. & Ammerer, G. Forkhead-like transcription factors recruit Ndd1 to the chromatin of G2/M-specific promoters. *Nature* **406**, 94–8 (2000).

[17] Kumar, R. *et al.* Forkhead transcription factors, Fkh1p and Fkh2p, collaborate with Mcm1p to control transcription required for M-phase. *Current Biology* **10**, 896–906 (2000).

[18] Lydall, D., Ammerer, G. & Nasmyth, K. A new role for MCM1 in yeast: cell cycle regulation of SW15 transcription. *Genes and Development* **5**, 2405–2419 (1991).

[19] Pramila, T., Miles, S., GuhaThakurta, D., Jemiolo, D. & Breeden, L. Conserved homeodomain proteins interact with MADS box protein Mcm1 to restrict ECB-dependent transcription to the M/G1 phase of the cell cycle. *Genes & Development* **16**, 3034–3045 (2002).

[20] Costanzo, M. *et al.* CDK activity antagonizes Whi5, an inhibitor of G1/S transcription in yeast. *Cell* **117**, 899–913 (2004).

[21] de Bruin, R., McDonald, W., Kalashnikova, T., Yates, J. & Wittenberg, C. Cln3 activates G1-specific transcription via phosphorylation of the SBF bound repressor Whi5. *Cell* **117**, 887–898 (2004).

[22] Li, C. & Wong, W. Model-based analysis of oligonucleotide arrays: Expression index computation and outlier detection. *Proceedings of the National Academy of Sciences* **98**, 31–36 (2001).

[23] Gentleman, R. C. *et al.* Bioconductor: Open software development for computational biology and bioinformatics. *Genome Biology* **5**, R80 (2004).

[24] Ihaka, R. & Gentleman, R. R: A language for data analysis and graphics. *Journal of Computational and Graphical Statistics* **5**, 299–314 (1996).

[25] de Lichtenberg, U. *et al.* Comparison of computational methods for the identification of cell cycle-regulated genes. *Bioinformatics* **21**, 1164–1171 (2005).

[26] Frey, B. & Dueck, D. Clustering by passing messages between data points. *Science* **315**, 972–976 (2007).

[27] Storey, J. A direct approach to false discovery rates. *Journal of the Royal Statistical Society, Series B (Statistical Methodology)* **64**, 479–498 (2002).

[28] Koch, C., Moll, T., Neuberg, M., Ahorn, H. & Nasmyth, K. A role for the transcription factors Mbp1 and Swi4 in progression from G1 to S phase. *Science* **261**, 1551–1557 (1993).

[29] Wittenberg, C. & Reed, S. Cell cycle-dependent transcription in yeast: promoters, transcription factors, and transcriptomes. *Oncogene* **24**, 2746–2755 (2005).

[30] Fisher, R. *Statistical methods for Research Workers* (Oliver and Boyd, 1932), fourth edn.

Table legends for Supplementary Table 1 and Supplementary Table 2

Table S1 | **Analysis results for periodic genes.** Each row corresponds to a particular Affymetrix probe (Column 2), identified as periodic (periodicity rank is in Column 3), mapped to a gene name (Column 1). The mapping is not one-to-one, as there are four cases in the table of two probes mapping to the same gene (numbers reported in the manuscript are given in terms of unique genes, not probes). The position of each gene/probe in Fig. 1 (Column 4) and Fig. 4 (Column 5) is provided where applicable. The PCS (Column 6) and ACS (Column 7) scores are shown, as well as a flag (Column 8) indicating if this gene/probe was identified as being different. The wild-type cluster (Column 9) and cyclin-mutant subcluster (Column 10) indices are provided where applicable. The average wild-type (Column 11) and cyclin-mutant (Column 12) PTRs, as well as the ratio between the two (Column 13) are also provided. Genes/probes identified as different but without cluster assignments were assigned to clusters that were later removed by filtering (Item 26).

Table S2 | **Analysis results for consensus periodic set (WTCON).** Each row corresponds to a particular Affymetrix probe (Column 2), mapped to a gene name (Column 1), for the 440 genes identified as periodic in this study (periodicity rank is in Column 3) as well as in the Pramila et al.[1] and Spellman et al.[2] studies (WTCON). The position of each gene in Supplementary Fig. 3 (Column 4) and Supplementary Fig. 10 (Column 5) is provided where applicable. The PCS (Column 6) and ACS (Column 7) scores are shown, as well as a flag (Column 8) indicating if this gene was identified as being different. The wild-type cluster (Column 9,11) and cyclin-mutant subcluster (Column 10,12) indices for Supplementary Figs. 15 and 18, respectively, are provided where applicable. The average wild-type (Column 13) and cyclin-mutant (Column 14) PTRs, as well as the ratio between the two (Column 15) are also provided. Genes identified as different but without cluster assignments were assigned to clusters that were later removed by filtering.

	Fig. 3	Supplementary Fig. 15	Supplementary Fig. 17
Total genes clustered	513	253	225
Percentage of initial genes clustered	61.4	82.4	100
Wild-type clusters	30	11	9
Cyclin-mutant clusters	56	26	13
Average Pearson correlation within wild-type cluster	0.808	0.880	0.874
Average Pearson correlation within cyclin-mutant cluster	0.790	0.817	0.832
Average Pearson correlation between wild-type and cyclin mutant	0.178	0.326	0.774
Average PTR within wild-type cluster	1.978	3.151	2.667
Average PTR within cyclin-mutant cluster	2.242	2.716	2.343
Average PTR ratio between wild-type and cyclin mutant	1.204	1.068	0.974

Table S3 | **Selected statistics of wild-type and cyclin-mutant clusters from Fig. 3 and Supplementary Figs. 15 and 18.** Each row corresponds to a particular statistic calculated on the appropriate clusters from Fig. 3 (Column 2), Supplementary Fig. 15 (Column 3), or Supplementary Fig. 17 (Column 4). The number of genes in the final clusters are given as a count (Row 1) and as a percentage of the total starting set (Row 2). This is not always 100% because genes can be lost during cyclin-mutant subcluster filtering. The number of wild-type clusters (Row 3) and cyclin-mutant subclusters (Row 4) in each clustering are provided. The average Pearson correlation between all genes within a wild-type cluster (Row 5) or cyclin-mutant (Row 6) subcluster are provided. The average wild-type to cyclin-mutant Pearson correlation (Row 7) and PTR ratio (Row 10) across all clustered genes is shown. The average PTR for all genes within a given wild-type cluster (Row 8) or cyclin-mutant subcluster (Row 9) are also provided.

WT Cluster	MT Cluster	Over-represented TFs with Q-Value ≤ 0.005
A	-	
A	1	
B	-	
B	2	
C	-	
C	3	
D	-	RLM1
D	4	
D	5	
E	-	SWI6,MBP1,STB1,SWI4,TEC1
E	6	SWI6,MBP1,SWI4
E	7	
E	8	STB1,TEC1,SWI4,SWI6
F	-	
F	9	SWI4
F	10	
F	11	MET31
F	12	
F	13	
G	-	
G	14	
G	15	
H	-	
H	16	
H	17	
I	-	
I	18	SWI6,SWI4
I	19	
I	20	
J	-	
J	21	
K	-	FKH1,FKH2
K	22	FKH1
K	23	
L	-	FKH1,SPT23,FKH2,YOX1
L	24	
L	25	
L	26	FKH1
M	-	FKH2,SMP1,NDD1,RLM1,SWI6,SWI4
M	27	
M	28	FKH2,NDD1,SWI6,RLM1,SWI4
N	-	
N	29	
O	-	NDD1,FKH2,MCM1,FKH1
O	30	NDD1,FKH2,MCM1,FKH1
O	31	
P	-	
P	32	
Q	-	
Q	33	
Q	34	
R	-	
R	35	
S	-	
S	36	
T	-	
T	37	
U	-	
U	38	
U	39	
V	-	YOX1,SWI5
V	40	YOX1
V	41	
V	42	SWI5
V	43	
W	-	YOX1,MCM1,HIR2,DIG1,ACE2,SWI5
W	44	YOX1,MCM1,HIR2,DIG1,ACE2,SWI5
X	-	ARR1
X	45	ARR1
Y	-	SWI4
Y	46	
Y	47	
Z	-	SWI5,ACE2
Z	48	SWI5
Z	49	
AA	-	
AA	50	
AA	51	
AB	-	SWI5,RME1,RLR1,ACE2,SPT2,NDD1,MBP1,SWI4,UME6
AB	52	SWI5,RME1,RLR1,ACE2,SPT2,NDD1,MBP1,SWI4,UME6
AC	-	
AC	53	
AC	54	
AD	-	
AD	55	
AD	56	

Table S4 | **Over-represented transcription factors in Fig. 3 by cluster/subcluster.** Each row corresponds to a wild-type cluster (indexed by letters A-AD) and cyclin-mutant subcluster (indexed by numbers 1-56) from Fig. 3. Each cell of the table—for the genes in the corresponding cluster or subcluster—contains the TFs with q-values ≤ 0.005, sorted from most to least significant.

a Literature Evidence

From	To	pVal	1	1b	2	3	4	5	6	7	8	9	10	11	12	13	14	15	16	17	18
ACE2	CLN3	2.6E-05	4.3E-02	1.7E-01		2.0E-03		2.0E-03			9.2E-04										
CLN3	MBP1																			√	√
CLN3	SWI4																			√	√
CLN3	SWI6																			√	√
FKH1	ACE2	1.3E-06	2.4E-05			4.7E-05		4.7E-05			1.5E-03										
FKH1	SWI5	1.2E-02	1.3E-02			1.7E-02		1.7E-02			9.3E-02				√	√	√	√			
FKH2	ACE2	2.6E-19‡	3.5E-07	8.9E-07		<1.0E-15‡		<1.0E-15‡			5.5E-06		√	√							
FKH2	SWI5	1.1E-12	3.2E-05	4.9E-04		9.4E-11		9.4E-11			3.5E-04	√	√	√	√	√	√	√			
HCM1	FKH1									√											
HCM1	FKH2									√											
HCM1	NDD1									√											
MBP1	HCM1	1.2E-19	1.6E-05		√	2.3E-14	√	2.3E-14			1.1E-07										
MBP1	YHP1	3.3E-09	8.8E-05			8.8E-07		8.8E-07			1.6E-04										
MBP1	YOX1	1.1E-10	1.5E-04			3.8E-07		3.8E-07			1.1E-05										
NDD1	ACE2	2.7E-21‡	3.2E-06	5.0E-05		<1.0E-15‡		<1.0E-15‡			5.1E-08			√							
NDD1	SWI5	3.7E-20†	8.0E-06	6.3E-04		<1.0E-15‡		<1.0E-15‡			7.5E-07			√	√	√		√			
SWI4	HCM1	2.8E-18	2.8E-06	2.0E-07	√	7.6E-13	√	7.6E-13	√		8.2E-08										
SWI4	NDD1	5.9E-12	1.2E-04	9.5E-07		1.9E-08	√	1.9E-08	√		1.0E-05										
SWI4	YHP1	7.2E-17	2.7E-06	1.2E-06	√	8.6E-12	√	8.6E-12	√		2.0E-07										
SWI4	YOX1	2.9E-15	2.4E-05	2.0E-04	√	1.7E-10	√	1.7E-10	√		4.5E-07										
SWI5	CLN3	9.6E-04	5.8E-05	1.0E+00		7.3E-02		7.3E-02			1.3E-03										
SWI6	HCM1	9.8E-06	6.3E-03	1.3E-06		4.5E-05		4.5E-05			1.4E-02										
SWI6	NDD1	3.7E-10	3.1E-04	8.6E-05		1.8E-07		1.8E-07			7.8E-05										
SWI6	YHP1	4.0E-21	2.4E-06	2.2E-05		3.8E-15		3.8E-15			2.1E-08										
SWI6	YOX1	1.8E-20	9.0E-06	1.8E-03		1.5E-14		1.5E-14			2.4E-08										
YHP1	CLN3	7.8E-01				7.7E-01													√		
YHP1	SWI4	5.2E-01				5.2E-01													√		
YOX1	CLN3	2.6E-01				2.6E-01													√		

b Literature Sources

pVal	Combined p-values from Lee et al. and Simon et al. using Fisher's method
1*	Workman CT et al, Science, 2006; 312(5776):1054-59 *WT*
1b**	Workman CT et al, Science, 2006; 312(5776):1054-59 *MMS*
2	Bean JM et al. Genetics. 2005 Sep; 171(1):49-61
3†	Harbison CT et al. Nature, 2004 Sep 2;431(7004);99-104
4	Iyer VR et al. Nature. 2001 Jan 25;409(6819):533-8
5††	Lee TI et al., Science, 2002; 298(5594):799-804
6	Horak CE et al. Genes Dev, 2002; 16(23);3017-33
7	Pramila et al. Genes and Development, 2006; 20(16):2266-2278
8†††	Simon I et al. Cell, 2001; 6(6):697-708
9	Zhu G et al., Nature, 2000 Jul 6;406(6791):90-4
10	Pic A et al. EMBO J, 2000;9(14):3750-61
11	Pic-Taylor A et al., Mol Cell Biol, 2004 Nov;24(22):10036-46
12	Althoefer H et al. Mol Cell Biol, 1995; 15(11):5917-28
13	Koranda M et al., Nature, 2000 Jul 6;406(6791):94-8
14	Kumar R et al., Curr Biol, 2000;0(15):896-906
15	Lydall D et al. Genes Dev, 1991 Dec;5(12):2405-19
16	Pramila T et al. Genes Dev, 2002; 6(23):3034-45
17	Costanzo M et al. Cell, 2004;117:899-913
18	de Bruin R et al. Cell 2004; 117: 887-898

* http://chianti.ucsd.edu/Workman_Mak2006/tables/BLA_YPD_pvalues.tab

** http://chianti.ucsd.edu/Workman_Mak2006/tables/BLA_MMS_pvalues.tab

† http://jura.wi.mit.edu/young_public/regulatory_code/files_for_paper_abbr.zip : pvalbygene_forpaper_abbr.xls

†† http://jura.wi.mit.edu/young_public/regulatory-network/Results_updated%20_1206003.zip : 106_pvalbygene_EF_ypd_v9.0.xls

††† http://jura.wi.mit.edu/young_public/cellcycle/all_genes.tsv

‡ A p-value of 1.0E-15 was substituted for the p-value of 0 reported in Lee et al.

Table S5 | **Literature evidence for regulatory interactions in Fig. 4c. a**, Each row corresponds to a regulatory interaction (or a component of a regulatory interaction in the case of complexes) in the Fig. 4c model architecture. Each numbered column corresponds to a different study in the literature. Green boxes represent high-confidence evidence for the regulatory interaction. P-values are reported where available, and p-values≤ 0.001 were considered high-confidence. The p-values reported in Simon et al.[11] and Lee et al.[9] were the result of independent experiments (Tony Lee, personal communication, December 12, 2007), and the pVal column is a composite p-value calculated using Fisher's method.[30] **b**, Each row defines the source of the data presented in the corresponding column in (**a**). Footnotes denote exact data sources where appropriate.

a Initial Regulatory Logic Choice

TF	Activation Rule
MBF	CLN3
SBF	(CLN3 ∨ MBF) ∧ ¬(YOX1 ∧ YHP1)
YOX1	MBF ∧ SBF
HCM1	MBF ∧ SBF
YHP1	MBF ∨ SBF
SFF	SBF ∧ HCM1
ACE2	SFF
SWI5	SFF
CLN3	(SWI5 ∧ ACE2) ∧ ¬(YOX1 ∧ YHP1)

b Attractor Distributions

Repressor	SFF	CLN3	All Off	Cycle 1	Cycle 2	Cycle 3
(YOX1 ∧ YHP1)	SBF ∧ HCM1	SWI5 ∧ ACE2	19.7%	80.3%	0%	0%
(YOX1 ∧ YHP1)	SBF ∧ HCM1	SWI5 ∨ ACE2	13.9%	86.1%	0%	0%
(YOX1 ∧ YHP1)	SBF ∨ HCM1	SWI5 ∧ ACE2	3.3%	0%	0%	96.7%
(YOX1 ∧ YHP1)	SBF ∨ HCM1	SWI5 ∨ ACE2	2.1%	0%	0%	97.9%
(YOX1 ∨ YHP1)	SBF ∧ HCM1	SWI5 ∧ ACE2	76.6%	23.4%	0%	0%
(YOX1 ∨ YHP1)	SBF ∧ HCM1	SWI5 ∨ ACE2	79.7%	20.3%	0%	0%
(YOX1 ∨ YHP1)	SBF ∨ HCM1	SWI5 ∧ ACE2	34.8%	0%	45.3%	19.9%
(YOX1 ∨ YHP1)	SBF ∨ HCM1	SWI5 ∨ ACE2	38.7%	0%	45.3%	16.0%

c Cycle 1 (used to color Fig. 4c)

	S1	S2	S3	S4	S5
MBF	1	0	0	0	0
SBF	1	1	0	0	0
YOX1	0	1	0	0	0
HCM1	0	1	0	0	0
YHP1	0	1	1	0	0
SFF	0	0	1	0	0
ACE2	0	0	0	1	0
SWI5	0	0	0	1	0
CLN3	0	0	0	0	1

d Cycle 2

S1	S2	S3	S4	S5
1	0	0	0	0
1	1	0	0	0
0	1	0	0	0
0	1	0	0	0
0	1	1	0	0
0	1	1	0	0
0	0	1	1	0
0	0	1	1	0
0	0	0	0	1

e Cycle 3

S1	S2	S3	S4	S5
1	1	0	0	0
1	1	0	0	0
0	1	1	0	0
0	1	1	0	0
0	1	1	0	0
0	1	1	1	0
0	0	1	1	1
0	0	1	1	1
1	0	0	0	1

Table S6 | **Synchronously updating Boolean model describing the periodic transcription in cyclin-mutant cells. a**, An initial choice of a set of Boolean logic functions on the variables which produce the five state oscillating attractor referred to as Cycle 1. **b**, The percentages of all possible starting states that end in the four identified attractors for all simple functions of the activating logic rules for the repressive inputs to CLN3 and SBF (YOX1 and YHP1), and activators of SFF (SBF and HCM1), and CLN3 (SWI5 and ACE2) variables. **c**, The on/off states of the transcription factors (TFs) in the Cycle 1 attractor as used to color Fig. 4c and shown in Supplementary Fig. 12b. **d**, The on/off states of the TFs in the Cycle 2 attractor as shown in Supplementary Fig. 12c. **e**, The on/off states of the TFs in the Cycle 3 attractor as shown in Supplementary Fig. 12d.

Experiment	μ_0	δ	σ_0	σ_v	λ	β
Wild-type replicate 1	95.8 (93.2,98.2)	41.4 (37.1,45.4)	15.3 (14.2,16.4)	0.06 (0.04,0.08)	77.1 (73.4,80.9)	0.14 (0.12,0.17)
Wild-type replicate 2	100.3 (96.8,103.3)	35.1 (28.7,40.7)	20.8 (19.8,21.8)	0.05 (0.04,0.07)	85.0 (80.6,89.9)	0.18 (0.15,0.21)
Cyclin-mutant replicate 1	95.6 (94.4,96.9)	0	11.2 (9.4,13.1)	0.15 (0.14,0.16)	120.1 (118.1,122.1)	0.15
Cyclin-mutant replicate 2	89.3 (87.7,90.9)	0	23.0 (21.2,24.9)	0.13 (0.11,0.14)	114.8 (112.8,116.7)	0.15

Table S7 | **CLOCCS parameter estimates. Each row corresponds to a different arrest-release experiment.** The observed budding curves, as well as the model predictions for each experiment, are shown in Supplementary Fig. 14. Each cell contains the mean value for that column's parameter, given 250,000 iterations of the Markov chain used to fit that row's experiment. Below each mean is the 95% confidence range for that parameter in that experiment. Since the values of β and δ were fixed to be 0.15 and 0, respectively, when fitting CLOCCS in the cyclin-mutant experiments, no confidence intervals exist for these parameters in those experiments.

WT Cluster	MT Cluster	Over-represented TFs with Q-Value ≤ 0.005
A	-	SWI4,MBP1,RLM1,SWI6,PHD1,SWI5
A	1	
A	2	MBP1,SWI6,SWI4
B	-	SWI6,SWI4,STB1,MBP1,TEC1,STE12
B	3	SWI6,MBP1,SWI4,STB1,STE12,YNR063W,TEC1
B	4	STB1,SWI4,SWI6,MBP1,TEC1
B	5	SWI4,SWI6
C	-	HIR2,HIR1,HIR3,SWI4,HMS2,MBP1,SWI6
C	6	SWI6,SWI4
C	7	
C	8	HIR2,HIR1,HIR3
D	-	FKH2,FKH1,SWI6,MSN4,NDD1,SWI4
D	9	FKH2,FKH1
D	10	
D	11	FKH2,NDD1
E	-	NDD1,FKH2,MCM1,FKH1,SUM1,STB2
E	12	FKH2,MCM1,NDD1,FKH1
E	13	NDD1,FKH2,FKH1,MCM1
F	-	NDD1,FKH2
F	14	NDD1,FKH2
G	-	NDD1,FKH2,MCM1,YOX1
G	15	NDD1,FKH2,YOX1,MCM1
G	16	NDD1
H	-	
H	17	
H	18	
H	19	
I	-	SWI5,MCM1,RLM1
I	20	
I	21	
I	22	SWI5
I	23	SWI5
J	-	MCM1,YOX1,SWI5,ACE2,DIG1,SUT1,TEC1,RLM1,UGA3,DAL80,SWI4,HIR2, PHD1,YAP6,CUP9,MBP1,STE12,NRG1,CIN5,RPN4,SWI6,FKH1
J	24	MCM1,SWI5,YOX1,ACE2,DIG1,TEC1,SWI4,MBP1,RLM1,STE12,RPN4,PHD1, YAP6,SUT1,SWI6,CIN5,FKH1
J	25	
K	-	MBP1,SWI4,SWI6
K	26	MBP1,SWI4,SWI6

Table S8 | **Over-represented transcription factors in Supplementary Fig. 15 by cluster/subcluster.** Each row corresponds to a wild-type cluster (indexed by letters A-K) and cyclin-mutant subcluster (indexed by numbers 1-26) from Supplementary Fig. 15. Each cell of the table, for the genes in the corresponding cluster or subcluster, contains the TFs with q-values ≤ 0.005, sorted from most to least significant.

WT Cluster	MT Cluster	Over-represented TFs with Q-Value ≤ 0.005
A	-	MBP1,SWI6,SWI4,CBF1,RLM1,SKN7
A	1	MBP1,CBF1
A	2	MBP1,SWI6,SWI4
B	-	MBP1,SWI6,STB1,SWI4
B	3	MBP1,SWI6
B	4	STB1
B	5	MBP1,SWI6,SWI4,STB1
C	-	SWI6,MBP1,SWI4
C	6	SWI6,MBP1
C	7	SWI4
D	-	SWI6,SWI4,MBP1,HIR1,HIR2,YAP1,FKH2,HMS2,MCM1
D	8	SWI6,SWI4,MBP1,HIR1,HIR2,YAP1,FKH2,HMS2,MCM1
E	-	FKH2,FKH1
E	9	FKH2,FKH1
F	-	FKH2,NDD1,FKH1,MCM1
F	10	FKH2,NDD1,FKH1,MCM1
G	-	SWI5
G	11	SWI5
H	-	NDD1,SWI4,MBP1,SWI6,ACE2,SWI5
H	12	NDD1,SWI4,MBP1,SWI6,ACE2,SWI5
I	-	
I	13	

Table S9 | **Over-represented transcription factors in Supplementary Fig. 17 by cluster/subcluster.** Each row corresponds to a wild-type cluster (indexed by letters A-I) and cyclin-mutant subcluster (indexed by numbers 1-13) from Supplementary Fig. 17. Each cell of the table, for the genes in the corresponding cluster or subcluster, contains the TFs with q-values ≤ 0.005, sorted from most to least significant.